Hydrometallurgy 228 (2024) 106356

Contents lists available at ScienceDirect

Hydrometallurgy

journal homepage: www.elsevier.com/locate/hydromet

Identification of processes in Cu-ore heap leaching using Cu isotopes and leachate chemistry at Tschudi mine, northern Namibia

Ondra Sracek [a,*], Vojtěch Ettler [b], Martin Mihaljevič [b], Bohdan Kříbek [c], Ben Mapani [d], Vít Penížek [e], Tereza Zádorová [e], Aleš Vaněk [e]

[a] Department of Geology, Faculty of Science, Palacky University, 17. listopadu 12, 771 46 Olomouc, Czech Republic
[b] Institute of Geochemistry, Mineralogy and Mineral Resources, Faculty of Science, Charles University, Albertov 6, 128 00 Praha, Czech Republic
[c] Czech Geological Survey, Klárov 3, Praha 118 21, Czech Republic
[d] Department of Civil, Mining and Process Engineering, Namibia University of Science and Technology, Windhoek, Namibia
[e] Department of Soil Science and Soil Protection, Faculty of Agrobiology, Food and Natural Resources, Czech University of Life Sciences Praha, Kamýcká 129, 165 00 Praha 6, Czech Republic

ARTICLE INFO

Keywords:
Heap leaching
Copper isotopes
Fractionation
Leachate geochemistry

ABSTRACT

Copper isotopic fractionation (in $\delta^{65}Cu$) and leachate characterization were studied in the context of heap leaching at the Tschudi copper mine in northern Namibia. The leached solution is of Mg-SO_4 type with high Al and Fe concentrations. The source of Mg and Al in the leachate can be from the alteration of micas such as Mg-bearing muscovite confirmed by X-ray diffraction and scanning electron microscopy; however, the source of Mg cannot be determined with certainty. The principal secondary minerals identified in the leached ore are gypsum and jarosite. The value of pH in leachate is ~1.21 and the concentration of dissolved Cu, occurring mostly as $CuSO_4^0$ and Cu^{2+}, is about 2 g/L. In comparison with unleached ore (avg. $\delta^{65}Cu$ −1.47 ‰), leached ore exhibits lighter isotopic values (avg. $\delta^{65}Cu$ −6.01 ‰) with apparent isotopic fractionation $\Delta^{65}Cu_{\text{leached ore-unleached ore}}$ of about −4.54 ‰. In contrast, there is isotopic enrichment of leachate in heavier ^{65}Cu isotope (leachate $\delta^{65}Cu$ 0.34 ‰) with apparent isotopic fractionation $\Delta^{65}Cu_{\text{leachate-unleached ore}}$ value of +1.81 ‰. These results are in good agreement with Cu isotopic fractionation and depletion in heavier ^{65}Cu isotope reported for dissolution experiments in laboratory and groundwater linked to the porphyry copper ore deposits around the world. The leaching of heaps can be considered an analogy of upper part of gossans, but here the supergene enrichment zone is missing due to extremely low pH and oxidizing conditions.

1. Introduction

Heap leaching is a technology based on the percolation of a leaching solution through artificially created heaps of mined material. Leaching solutions encounter ore minerals in the mined material and dissolves them such that the pregnant leaching solution is collected at the bottom with collection pipes. Principal chemicals used in the leaching process are cyanides for gold extraction and sulfuric acid for the extraction of copper (Cu) and other base metals, (Petersen, 2016), while alkalis may be used for uranium, e.g., at Langer Heinrich mine, Namibia. There are several factors affecting the efficiency of leaching, e.g., size/specific surface area of the leached material (Lwambiyi et al., 2009), and its tortuosity (Maghsoudy et al., 2022). The composition of gangue rock is also very important factor, e.g., high content of carbonates can make leaching nearly impossible (Thomas, 2021). In the case of Cu, the pregnant leach solution (PLS) is further treated using organic extractants dissolved in solvents such as kerosine, strong acids and then ultrapure copper is obtained by the application of electrowinning with cathode Cu as a resulting product (Watling, 2006).

The Cu isotopes experience significant fractionation in many geochemical reactions (e.g., Albarède, 2004; Mathur et al., 2005; Bullen and Walczyk, 2009; Plumhoff et al., 2021; Majzlan et al., 2022) and have been used to trace sources of contamination and to describe dissolution/precipitation processes of Cu minerals, redox reactions, and adsorption (Bigalke et al., 2010; Wall et al., 2011; Wiederhold, 2015). In Namibia, the Cu isotopic tracing was used to identify sources of Cu in soils and grass shoots close to the Tsumeb smelter (Kříbek et al., 2018) and to determine the mobility of Cu in soils near the tailing disposal site of the

* Corresponding author.
E-mail address: srondra@seznam.cz (O. Sracek).

https://doi.org/10.1016/j.hydromet.2024.106356
Received 7 May 2024; Received in revised form 25 June 2024; Accepted 25 June 2024
Available online 4 July 2024

Kombat mine (Mihaljevič et al., 2019). Also, the changes in Cu isotopic composition indicated processes related to the weathering of copper porphyry ore deposits (Sarjoughian et al., 2024) and were used as an indicator of proximal copper deposits for mineral exploration purposes (Mahan et al., 2023).

In this study we collected and analyzed solid phases and leachates from the heap leaching process at the Tschudi copper mine site in northern Namibia, (Fig. 1a), and analyzed copper isotopes and leachate chemistry. To our knowledge, field studies of copper isotopic fractionation in heap leachate are missing in literature so far, but there are several laboratory Cu-ore leaching studies under controlled conditions, e.g., Mathur and Schlitt (2010), and Wall et al. (2011). The principal objectives of this study were (1) to furnish a description of copper isotopes fractionation during the leaching process in the field (i.e., at an active Cu heap leaching facility) and compare it with controlled laboratory experimental results, and (2) the determination of leachate chemistry with a special focus on Cu speciation.

2. Site description and leaching procedure

The Tschudi mine site is located in the north-central part of Namibia (Fig. 1a). It lies within a semiarid region with extremely seasonal precipitation of about 470 mm per year, which falls exclusively between October and March. Maximum temperatures reach 32 °C in October, (Van Wyk et al., 2001; Mendelsohn et al., 2002).

The Tschudi low-grade Cu deposit is located around 20 km west of Tsumeb, in the Oshikoto Region of Namibia, and occurs as the upper subgroup within the Otavi Supergroup. The deposit is located within the Tschudi Formation of the Mulden Group sediments which form a part of the Neoproterozoic Damara Belt (Schneider, 2008). The mined ores are hosted by basal sandstones with minor conglomerates that overstep barren carbonate sediments of the Tsumeb Subgroup. The primary ore

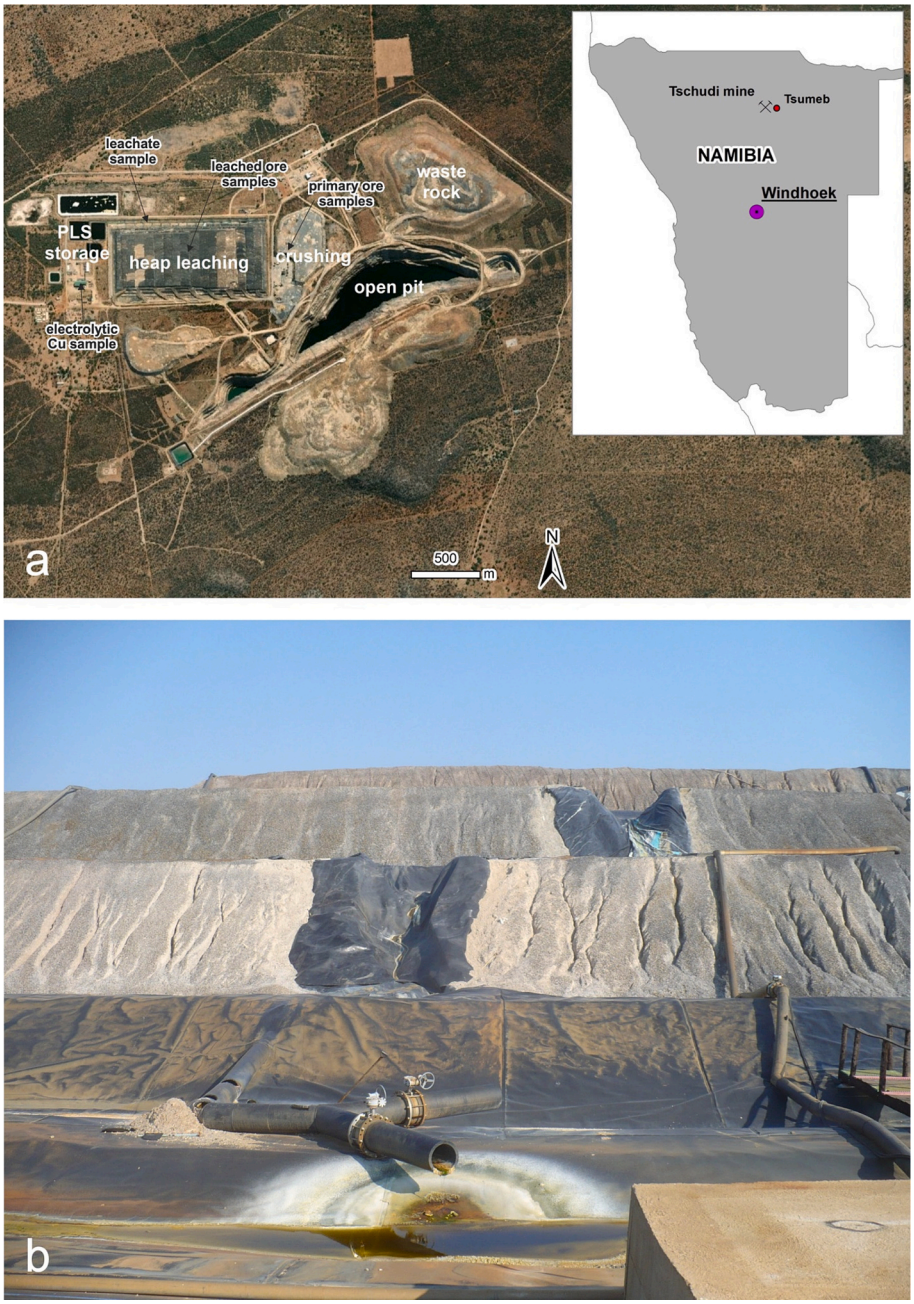

Fig. 1. (a) Location of Tschudi mine and sampling sites (see text), (b) Leaching waste rock pile; sampling of leachate was from the pipe in the middle.

consist of chalcocite, Cu_2S, bornite, Cu_5FeS_4, chalcopyrite, $CuFeS_2$, covellite, CuS, and minor pyrite, FeS_2. Currently mined oxidized ore consists of malachite, $Cu_2(OH)_2CO_3$, and minor azurite, $Cu_3(CO_3)_2(OH)_2$. The ore body is in the basal sandstone and conglomerate of the Mulden Group and its strike length reaches about 2500 m. The zone of oxidized copper mineralization reaches up to 70 m depth, and is composed mostly of malachite, and chalcocite and the deeper sulphidic zone contains mostly chalcocite and bornite.

The mineralization is exploited as an open pit mine, about 160 m deep using standard drill and blast methods followed by loading and trucking of mined rocks. The ore is blended by the finger pile system and goes through a primary jaw crusher, a secondary gyratory crusher, and two tertiary gyratory crushers, and finally reaching particles of 16–19 mm size range. After crushing, the ore is treated in an agglomeration plant where sulfuric acid and raffinate are added to the crushed material. Then, the agglomerated rock is deposited on the heap leach pad 6–8 m high and is leached by sulfuric acid solution applied at the rate of 6 L h^{-1} m^{-2}. After leaching, Cu leachate is collected in storage pond. The leachate contains about 2 g/L of Cu. The leachate is then extracted by a mixture of paraffin and kerosine. Finally, the pregnant solution is processed by electrowinning. The product is ultrapure cathodic Cu that is bundled and transported to the port terminal at Walvis Bay.

3. Material and methods

Solid phase samples for elemental Cu isotopic analyses were collected from the crusher of primary rock (samples T1A,B,C; T2, T5, T6) and from leached zone of the heap (samples T3, T7) and stored in plastic bags. A sample of metallic Cu (T4) was taken from the electrolytic cell (Fig. 1a) (list of samples is reported in Table S1 in the Supplementary Material).

The acid leachate (PLS – pregnant leach solution) was sampled at the outflow pipe at the base of leaching heap (Fig. 1b). The sample was filtered using B-Braun Omnific 20 mL syringes through a 0.45-μm Millex-HV PVDF Durapore filters (Millipore, USA) and measured for physico-chemical parameters: pH and redox potential were determined using a WTW Multi 3620 IDS multimeter equipped with a WTW SenTix® 940 pH electrode and a SenTix® ORP-T 900 redox electrode (WTW, Germany), calibrated against a set of WTW technical buffers, 2.00, 4.01 and 7.00 and a WTW RH28 redox standard (220 mV for Pt-Ag/AgCl at 25 °C), respectively; electric conductivity (EC) was measured using a Mettler-Toledo Seven2Go conductometer with a Mettler-Toledo InLab® 738 ISM conductivity probe (Mettler-Toledo, Switzerland) calibrated against a Hamilton Basic Line conductivity standard (1413 μS/cm at 25 °C). Major cations and total S and P in the leachate were determined using inductively coupled plasma optical emission spectrometry (ICP-OES Agilent 5110, USA) and trace elements (Ag, Al, As, Ba, Be, Bi, Br, Cd, Co, Cr, Cu, Fe, Li, Mo, Mn, Pb, Sb, Se, Sn, Sr, Tl, V, Zn) were analyzed with inductively coupled plasma quadrupole-based mass spectrometry (ICP-QMS Thermo Scientific, iCAP-Q™, Germany). The accuracy of the measurement was checked by the analysis of NIST 1643f certified reference material (for trace elements in water) (Table S2).

The aliquot parts of the solid samples were crushed using a jaw crusher and pulverized in a Retsch planetary mill PM 400 in agate jars. Preliminary bulk chemical analyses of the Tschudi sample materials were carried out by portable X-ray fluorescence spectrometer (pXRF) using a Thermo Scientific Niton XL3t Goldd instrument with Thermo Scientific sample holder and the AllGeo calibration mode. For further chemical and isotopic analyses, solid samples were dissolved in mineral acids using the following digestion procedure: 0.2 g of material was covered with 5 mL of concentrated HNO_3 in Teflon beakers (Savillex, USA) and heated for 24 h; the mixture was evaporated to near dryness and 5 mL of HF (38%) and 0.5 ml of $HClO_4$ (70%) were added in two cycles and heated on hot plate; the mixture was evaporated to near-dryness again and diluted in 2% HNO_3 (*v*/v). The concentrations of major and trace elements in the digests were determined using a combination of ICP-OES and ICP-QMS operated under standard analytical conditions. The CCU-1e (copper concentrate), CZN-4 (zinc concentrate) and SU-1b (nickel-copper-cobalt ore) certified reference materials released by the CCRMP-Canadian Certified Reference Materials project were used to check the accuracy of the digestion and analytical procedures (Table S2).

Selected ore samples were prepared as polished sections and examined using an electron microprobe microanalyzer (EPMA; JEOL JXA-8530F, Japan) equipped with a field emission gun electron source (FEG). We used this instrument for scanning electron microscopic (SEM) imaging and the energy dispersion spectroscopic (EDS) analyses (spectrometer JEOL JED-2300F).

The minerals in the primary and leached ore were determined using the X-ray powder diffraction analysis (XRPD). The samples were pulverized to analytical fineness in an agate mortar (Retsch PM 400 planetary mill, Germany) and analyzed either using a PANalytical X'Pert Pro diffractometer (PANalytical, the Netherlands) with an X'Celerator detector (CuKα radiation at 40 kV and 30 mA, 2 theta range of 2–80°, step of 0.02°, counting time of 150 s per step) or a Bruker D8 Advance diffractometer with Lynxeye XE detector (CuKα radiation, 2 theta range of 4–80°, step of 0.015°, counting time of 0.8 s per step). The X'Pert HighScore Plus 3.0 software coupled to the Crystallography Open Database (COD), (Gražulis et al., 2012), were used for analysis of the XRPD patterns. The data were plotted using a combination of Prism 10 (GraphPad, USA) and Graphic for Mac (Picta, USA) software packages.

The Cu sample for isotopic composition was separated from stock solutions prepared by ore digestion and from the leaching solution. The detailed procedure is given in Mihaljevič et al. (2019). Resin Ag1X8 in Poly-Prep chromatography columns (BioRad, Cl form, 200–400 mesh) was cleaned with 20 mL of 2% HNO_3 and subsequently conditioned with 20 mL of 6 M HCl. An aliquot containing at least 500 ng of Cu was evaporated to near dryness in a Savillex vessel and then dissolved in concentrated HCl. The samples were repeatedly evaporated and then dissolved in 1 mL of 6 M HCl with 0.001% H_2O_2 for subsequent loading onto the column. Subsequently, the matrix was eluted with 4 mL of 6 M HCl and another 4 mL of 5 M HCl; Cu was eluted with 20 mL of 5 M HCl. The column was then cleaned with 2% HNO_3.The separation was repeated if the yield of separated Cu differed by >5% from the original separated load. The resulting solution was analyzed using a Neptune Plus multi-collector inductively coupled plasma mass spectrometer (MC ICP-MS, Thermo Fisher Scientific, Germany). Mass bias drift was corrected by the addition of SRM 986 (Ni isotopic standard, NIST USA) to the $^{62}Ni/^{60}Ni$ ratio. Further correction was made by bracketing to SRM 976 (Cu isotopic standard, NIST USA) and the resulting Cu isotopic composition was calculated as $\delta^{65}Cu$ (Eq. 1).

$$\delta^{65}Cu\ (‰) = \left[\left({}^{65}Cu/{}^{63}Cu \right)_{sample} \Big/ \left({}^{65}Cu/{}^{63}Cu \right)_{standard} - 1 \right] \text{ x } 1000 \qquad (1)$$

The procedural blank of the whole procedure was <5 ng. The results of external reproducibility for $\delta^{65}Cu$ of BCR-2 (Columbia River Basalt, USGS) certified reference material for the three replicates was 0.38 ± 0.06 (2SD), i.e., in an acceptable range (Chapman et al., 2006).

The chemicals and acids used for digestion and separation were of analytical grade. Acids (HF, HCl, and HNO_3) were subsequently sub-boiling distilled using a DST 1000 PFA device (Savillex, USA), and water for the preparation of solutions was obtained from a MilliQ+ device (Millipore, USA). All used plasma spectrometers are located in the laboratories of the Faculty of Science, Charles University.

The composition of leachate was used for speciation performed by the code PHREEQC-2 (Parkhurst and Appelo, 1999) using databases minteg.v4.dat and pitzer.dat. The data were plotted using a combination of Prism 10 (GraphPad, USA) and Graphic for Mac (Picta, USA) software packages.

4. Results

4.1. Solid phase mineralogy

Results of X-ray diffraction identification of phase compositions on selected solid sample are given in Fig. 2 and in Table S1. In the unleached ore, principal gangue minerals are quartz, calcite, feldspar, montmorillonite [$(Na,Ca)_{0.33}(Al,Mg)_2(Si_4O_{10})(OH)_2{\cdot}nH_2O$], and mica. The mica cannot be fully identified because the diffraction peak overlaps, but further scanning electron microscopy investigation confirmed the predominance of muscovite [$KAl_2(Si_3Al)O_{10}(OH,F)_2$]. Principal Cu-bearing minerals identified are bornite, Cu_5FeS_4, malachite, $Cu_2(OH)_2CO_3$, and azurite, $Cu_3(CO_3)_2(OH)_2$. In the leached ore samples, quartz dominates again, and there still are feldspar, montmorillonite, and mica. Secondary minerals such as gypsum and jarosite, which are not present in primary ore, appear in the leached ore.

Scanning electron micrographs are shown in Fig. 3 and total contents and results of EDS analyses are presented in Table S3. In unleached ore rich in sulfide minerals, principal minerals are chalcopyrite, pyrite, and covellite embedded in quartz and silicate matrix containing Mg-rich muscovite with Mg content up to 2.12 wt% (Table S3). Accessory minerals are apatite, and rutile (Figs. 3, ab). In the unleached ore rich in carbonates, there is malachite that has formed around primary sulfides such as chalcocite, covellite, and stromeyerite, AgCuS, also embedded in silicate matrix and there are veinlets of silica gel highly enriched in Cu (Fig. 3 cd). In leached ore, principal secondary minerals are jarosite and plumbojarosite, $PbFe_6^{3+}(SO_4)_4(OH)_{12}$, and they are accompanied by feldspar, quartz, and rutile (Fig. 3, ef). No gypsum was found in leached ore under SEM, but it was identified by X-ray diffraction (see Fig. 2).

4.2. Leachate chemistry and speciation

Chemical composition of leachate is presented in Table 1. The onsite parameters measured in the field and used in speciation calculation were as follows: temperature 27 °C, pH of 1.21; Eh 604 mV, EC was 136 mS/cm. The water (leachate) is of Mg-SO_4 type with very high Mg and SO_4 concentrations. Concentrations of Fe, Mn, and Al in leachate are also high, but lower than those of Mg and SO_4. As expected, concentration of target metal Cu is very high, >2 g/L, but concentrations of other trace metals are much lower.

Selected results of leachate speciation are shown in Table 2. There is a lack of Pitzer's parameters for several metals in leachate including Cu and for them a minteq.v4 database was used. However, results for other ions calculated with pitzer.dat database were similar for both databases.

Leachate is undersaturated with respect to all Cu minerals such as chalcanthite, $CuSO_4{\cdot}5H_2O$, and also with respect to all Al minerals such as alunite, $KAl_3(SO_4)_2(OH)_6$, and also with respect to melanterite, $FeSO_4{\cdot}7H_2O$. In contrast, supersaturation is reached for K-jarosite and H-

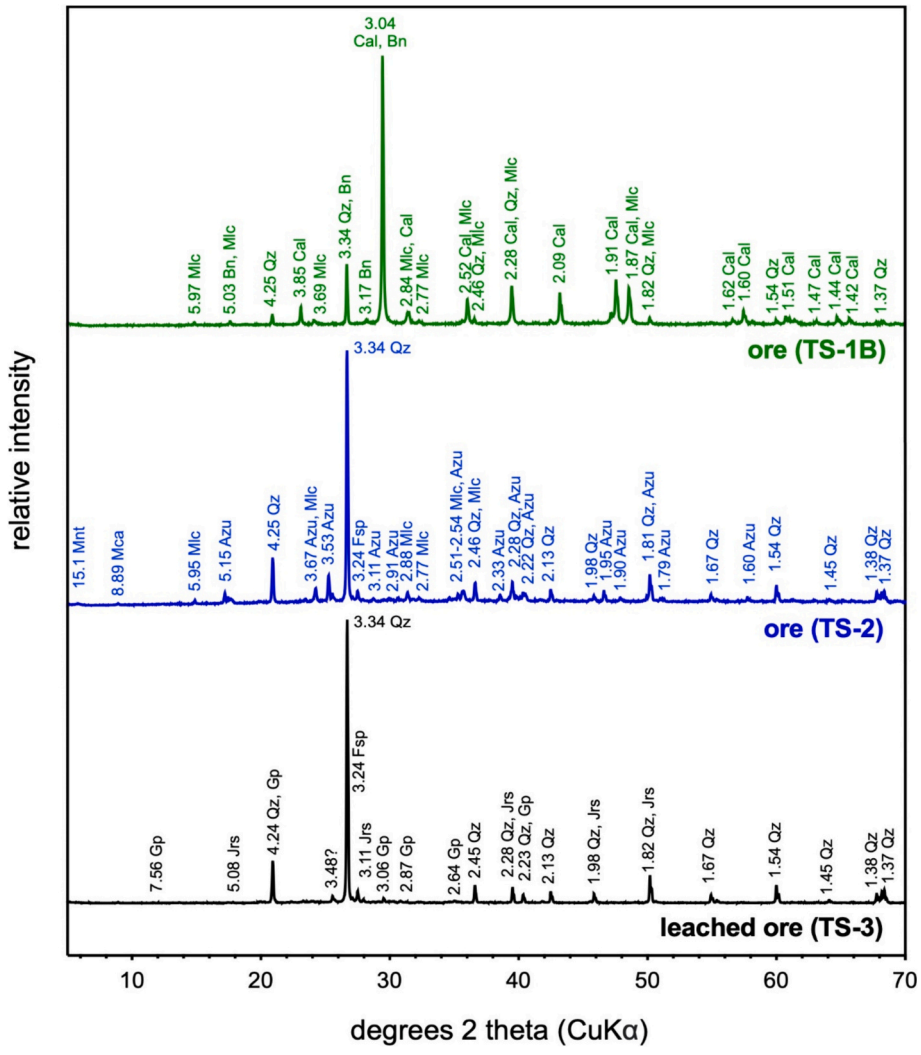

Fig. 2. Representative X-diffraction patterns for selected unleached ore samples (TS-1B, TS-2), and a leached ore sample (TS-3). Abbreviations: Cal- calcite, Qz - quartz, Mlc - malachite, Bn - bornite, Azu - azurite, Mca - mica, Mnt- montmorillonite, Gp - gypsum, Jrs - jarosite, Fsp - feldspar.

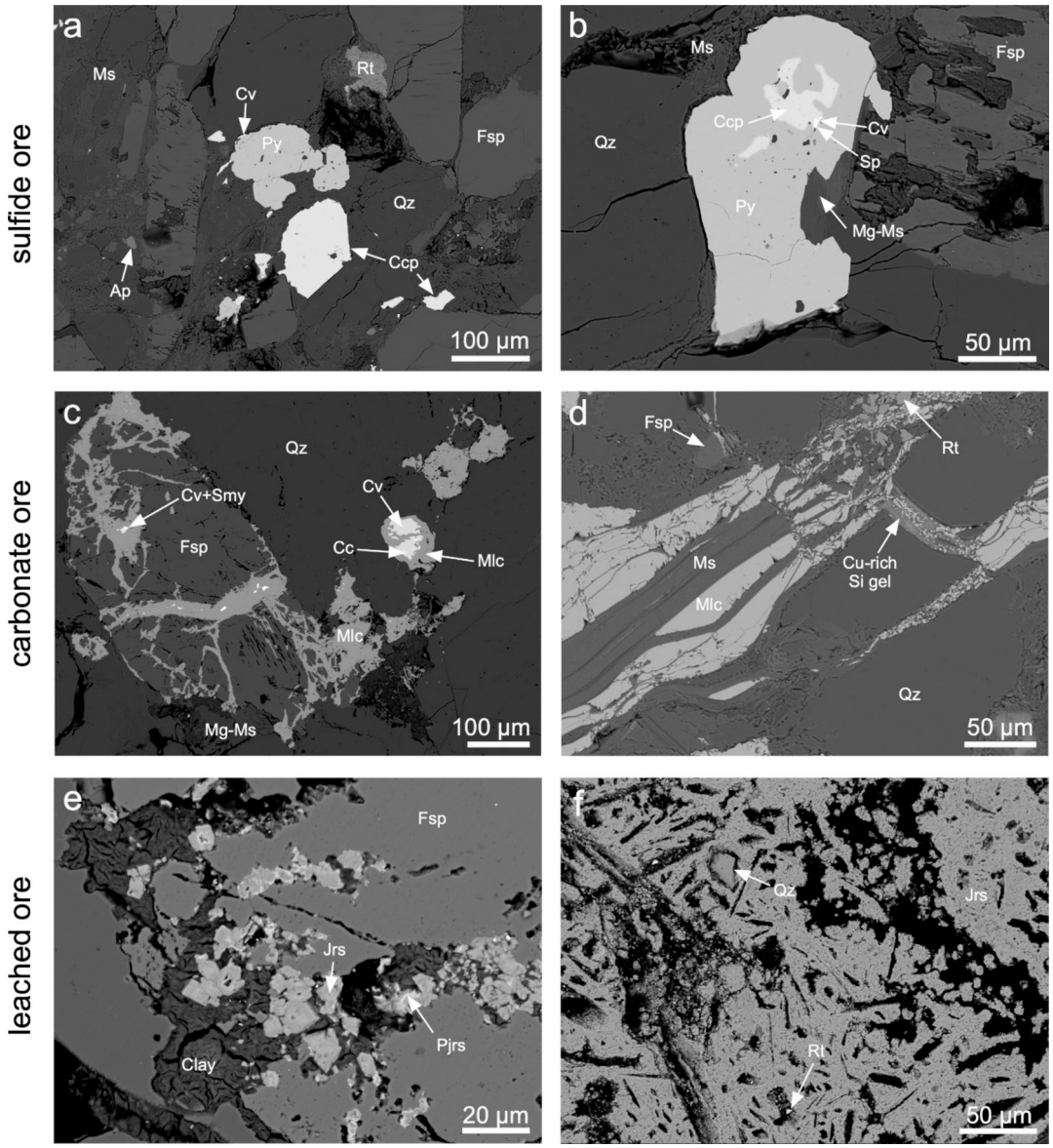

Fig. 3. Scanning electron micrographs in backscattered electrons (BSE) of unleached sulfidic ore (TS-5), unleached carbonate ore (TS-6, TS-1 A), and leached ore (TS-3) from Tschudi. (a) Grains of sulfides (chalcopyrite and pyrite with covellite layer) embedded in matrix composed of quartz, feldspar and muscovite with grains of other, accessory minerals (rutile, apatite) (sample TS-5); (b) Large pyrite grain with chalcopyrite, covellite and sphalerite inclusions located within the silicate matrix (quartz, feldspar, muscovite, Mg-bearing muscovite) (sample TS-5); (c) Secondary malachite forming weathering rims around primary sulfides (chalcocite, covellite, stromeyerite) and filling the veinlets in the silicate matrix composed of feldspar, quartz and Mg-bearing muscovite (sample TS-6); (d) Malachite veinlets associated with muscovite, feldspar and quartz, with accessory grains of rutile. Note the presence Cu-bearing silica gel filling some of the veinlets and containing up to 39 wt% Cu (sample TS-1 A); (e) Jarosite crystals with Pb-rich zones corresponding to plumbojarosite associated with feldspar and unidentified clay minerals (sample TS-3); (f) Jarosite aggregate with residual crystals of primary quartz and rutile (sample TS-3). Mineral abbreviations according to Warr (2021): Ap – apatite, Bn – bornite, Ccp – chalcopyrite, Cv – covellite, Fsp – feldspar, Gp – gypsum, Jrs – jarosite, Mlc – malachite, Ms. – muscovite, Mg-Ms – Mg-bearing muscovite, Pjrs – plumbojarosite, Qz – quartz, Smy – stromeyerite, Sp – sphalerite, Rt – rutile.

Table 1
Chemical composition of leachate, concentrations in mg/L.

pH	Electrical conductivity (EC) mS/cm	Concentration of ions (mg/L)													
		Na	K	Ca	Mg	Cl	SO_4	Al	Fe	Mn	Si	Zn	Cd	Pb	Cu
1.21	136	114	63	622	6044	176	76,992	2246	6675	1420	87	218	14	3.3	2137

jarosite. Despite very high Mg concentration, the leachate is also undersaturated with respect to epsomite, $MgSO_4{\cdot}7H_2O$ and other Mg sulfate minerals. Supersaturation is reached for gypsum and anhydrite and also for quartz and chalcedony. Speciation of Cu present in an oxidizing environment as Cu(II) is dominated by $CuSO_4^0$ (74.3%) and Cu^{2+} (25.5%).

The results indicate that Cu behaves conservatively in leachate, i.e., it does not precipitate and its adsorption at the measured pH < 2 is unlikely (Appelo and Postma, 2005). In contrast, sulfate concentration can be affected by gypsum and jarosite precipitation due to positive SI,

Table 2
Selected results of saturation indices (SI) for leachate.

Mineral	Gypsum	Chalcanthite	Alunite	K-jarosite	$Fe(OH)_3$	Melanterite	Quartz	Epsomite
Formula	$CaSO_4{\cdot}2H_2O$	$CuSO_4{\cdot}5H_2O$	$KAl_3(SO_4)_2(OH)_6$	$KFe_3(SO_4)_2(OH)_6$	$Fe(OH)_3$	$FeSO_4{\cdot}7H_2O$	SiO_2	$MgSO_4{\cdot}7H_2O$
Saturation index (SI)	0.27	−1.41	−8.34	2.14	−5.16	−4.20	1.20	−1.02

Note: If a solution is undersaturated with respect to a mineral in contact with the solution (i.e., SI is negative), then the mineral could dissolve if present, but it cannot precipitate.

but supersaturation with respect to Al- and Mg-minerals is not reached due to negative SI (Table 2).

4.3. Copper stable isotopes

Results of Cu isotopic analysis including standard deviations are shown in Table S4 and Fig. 4. For the unleached ore, $\delta^{65}Cu$ values of carbonate ore samples vary from −4.11 ‰ to 1.42 ‰ and sulfide ore sample has a value of −2.08 ‰. Average $\delta^{65}Cu$ of all unleached samples is −1.47 ‰. Values of $\delta^{65}Cu$ in leached ore samples vary from −8.17 ‰ to −3.87 ‰ (avg. -6.01 ‰). Value of $\delta^{65}Cu$ in leachate is +0.34 ‰ and value $\delta^{65}Cu$ of pure metallic Cu, produced by the electrolytical process, is +4.24 ‰.

The results imply apparent fractionation $\Delta^{65}Cu = \delta^{65}Cu_{lo} - \delta^{65}Cu_{uo} = -4.54$ ‰, where "lo" indicates leached ore and "uo" indicates unleached ore, i.e., there is a strong isotopic decrease in $\delta^{65}Cu$ values of primary unleached ore in leaching process. In contrast, there is an increase in $\delta^{65}Cu$ values of leachate with the value of $\Delta^{65}Cu = \delta^{65}Cu_{le} - \delta^{65}Cu_{uo} = +1.81$ ‰, where "le" stands for leachate.

5. Discussion

Principal Cu-minerals identified in the exploited ore are chalcocite, Cu_2S, bornite, Cu_5FeS_4, covellite, CuS, and malachite, $Cu_2(OH)_2CO_3$. Dissolution of malachite with copper as Cu(II) in acid solution is described as:

$$Cu_2(OH)_2CO_3 + 4H^+ = 2Cu^{2+} + CO_2 + 3H_2O \quad (2)$$

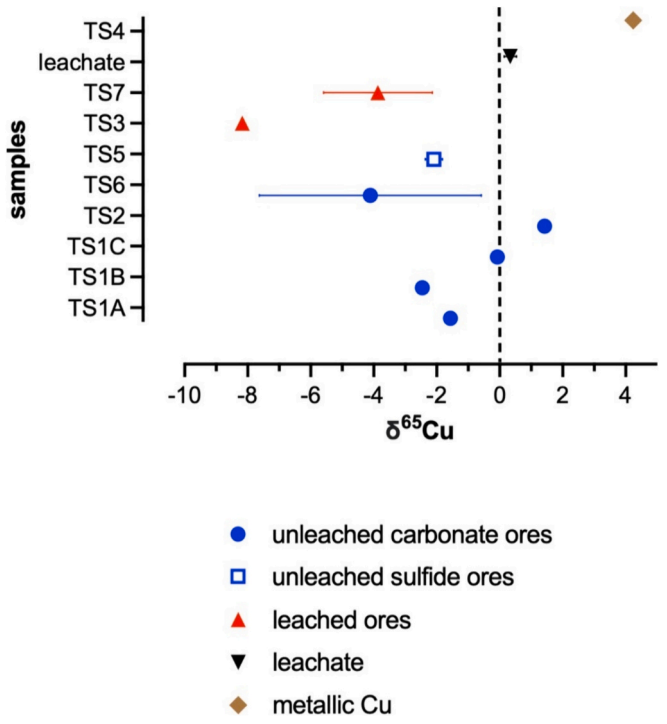

Fig. 4. Plot of $\delta^{65}Cu$ values, sample labels are in Table 3. Error bars are based on data in Table S4.

The rate-determining step was identified as chemical reaction on mineral surface (Nicol, 2018). However, a diffusion control was suggested for an early period of dissolution by Bingöl and Canbazoğlu (2004). Dissolution of bornite and chalcocite is more complex because there is oxidation of Cu present in ore as Cu(I), to Cu(II) along with the mineral dissolution. Oxidation agents can be both O_2 and Fe^{3+}, and the same applies to other Cu—Fe minerals such as bornite (Wall et al., 2011).

The leaching solution has very low pH of 1.21, consistent with low carbonate content in primary ore and gangue rock. Principal ions are Mg and SO_4, but there also are high concentrations of Fe, Mn, and Al. High Mg and Al concentrations can be a consequence of silicate minerals such as micas and chlorite dissolution (Sracek et al., 2004; Blowes et al., 2005; Appelo and Postma, 2005). Behavior of Al is conservative at pH < 4.2 and Al precipitates as $Al(OH)_3$ at higher pH, but Mg does not precipitate even at very low pH range except for extremely mineralized brines (Sracek et al., 2004). The potential source of Mg can be the dissolution biotite, $K(Mg,Fe)_3AlSi_3O_{10}(OH)_2$, and phlogopite, $KMg_3AlSi_3O_{10}(F,OH)_2$. The molar Al/Mg ratio in biotite and phlogopite is 1:3 or 0.33, and the same ratio of 0.336 is in leachate. Generally, biotite is dissolving incongruently and is later transformed to kaolinite, $Al_2Si_2O_5(OH)_4$, but further dissolution of kaolinite is already congruent (Hradil and Hostomský, 2002). However, no biotite or phlogopite have been found by EMPA, and the only Mg-bearing phase identified in ore before leaching was Mg-rich muscovite with Mg content up to 2.12 wt% (Fig. 3, Table S1). This seems to be a relatively low content, but assuming bulk density of heap material of about 1.8 kg/dm^3, porosity of about 0.3 (Lefebvre et al., 2001; Sracek et al., 2004), and 10% content of Mg-rich muscovite, 1 L of leaching solution is in contact with 6 kg of rock containing 12 g of Mg, which is much more than about 6 mg/L of Mg found in leachate (Table 1). However, this estimate is based on the assumption of constant Mg content and congruent dissolution, which may not be applicable in this case. This means that the source of Mg dominant in leachate cannot be determined with certainty.

Saturation indices (SI) for Al minerals are negative, (Table 2), and all Al produced by the dissolution of silicates is in the leachate. Dissolved Fe can precipitate as K-jarosite, $KFe_3(SO_4)_2(OH)_6$, as indicated by positive SI value for this mineral (Table 2). Bulk reaction for the oxidation of Fe^{2+} followed by the precipitation of K-jarosite is:

$$K^+ + 3Fe^{2+} + 0.75O_2 + 2SO_4^{2-} + 4.5H_2O = KFe_3(SO_4)_2(OH)_6 + 3H^+ \quad (3)$$

Thus, behavior of Fe in strongly acid solution can be non-conservative. The same applies to Ca which precipitates as gypsum, based on SI-value (Table 2) and also confirmed by mineralogical methods (Figs. 2, 3e and f).

At the Tschudi mine site, concentration of Cu in solution is about 2 g/L and speciation is dominated by $CuSO_4^0$ complex and free ion Cu^{2+}. Leachate is undersaturated with respect to all Cu minerals, i.e., the behavior of Cu in leachate is conservative, but saturation is reached with respect to anhydrite, gypsum, and quartz (Table 2).

Isotopically lighter composition of the leached rock was observed with value $\Delta^{65}Cu$ of 4.54 ‰ and, in contrast, isotopically heavier composition was observed with a value of $\Delta^{65}Cu$ of 1.81 ‰ in leachate. This is consistent with literature data, e.g., Mathur and Fantle (2015). One primary ore sample, TS2, has $\delta^{65}Cu$ value even slightly higher than the leachate, but this sample has large content of Cu(II) minerals such as

malachite and azurite (Table 3) and in this case isotopic fractionation caused by sulfide oxidation already before leaching was probably significant (Markl et al., 2006; Klein et al., 2010). Surprisingly, enrichment in $\delta^{65}Cu$ was also observed for metallic Cu produced in the galvanic process with $\delta^{65}Cu$ up to +4.24 ‰ (1 sample). This is puzzling because in this process Cu(II) is reduced to Cu(0) in metallic copper and isotopic depletion from −0.76‰ to −2.66 ‰ was observed under controlled laboratory conditions (Qi et al., 2019). However, analyzed metallic Cu from Tschudi site may not have been produced from the same leachate which was collected during our sampling because isotopic values of copper at Tschudi deposit are probably very heterogeneous and there is a possibility of its production from solution with different $\delta^{65}Cu$ value. Another possible explanation is the oxidation of the produced cathodic Cu(0) to Cu(II) during long time break in the cathodic copper production. The electrolytic tank was out of production for several months before sampling.

Increase in $\delta^{65}Cu$ values was also observed in other studies of Cu-minerals dissolution, e.g. (Fernandez and Borrok, 2009; Braxton and Mathur, 2011), but some results reported for abiotic vs. biotic dissolution were variable (Bullen and Walczyk, 2009). Nevertheless, some results reported for leaching of primary ores in natural leached zone of copper ores, i.e., gossans, were consistent. Gossans refer to highly ferruginous rocks formed through the oxidation of sulfide minerals by weathering and leaching. The Perkoa copper deposit in Burkina Faso, has a similar climate as the Tschudi mine site in Namibia; the gossan was isotopically depleted compared to the primary ore with a value of $\Delta^{65}Cu$ of −2.36 ‰ (Kříbek et al., 2016). Depletion of leached ore zone was also reported from the Kerman porphyry ore deposit in Iran, with similar climatic conditions as Tschudi. Average values of $\delta^{65}Cu$ in leached zone, supergene zone, and hypogene zone were 0.42 ‰, 7.17 ‰, and 4.36 ‰, respectively, Sarjoughian et al. (2024). Strong observed isotopic enrichment in supergene zone of gossan is caused by precipitation of secondary sulfides from isotopically enriched leaching solution (Mathur et al., 2005; Kim et al., 2019).

Compilation of data from copper ore deposits around the world confirmed a strong depletion ^{65}Cu isotope in leached zone and an enrichment in supergene zone compared to primary ore (Mathur and Fantle, 2015). Also, isotopic enrichment of $\delta^{65}Cu$ in groundwater was suggested as an indicative criterion for prospection of Cu ore deposits at Mt. Isa in Australia (Mahan et al., 2023). At this site, values of $\delta^{65}Cu$ in the proximity of Cu ore deposit are higher and decrease with distance, presumably as a consequence of isotopically heavier Cu adsorption. Thus, leached heaps can be considered as analogies of upper parts of gossans, but there is no development of supergene enrichment zone at the base due to a low pH and oxidizing conditions. Also, the rate of mineral dissolution in leached heaps is much faster compared to gossans because of relatively small and uniform grain size and a strong acid applied.

6. Conclusions

This study performed at the Tschudi copper mine site in north-central Namibia and combined mineralogical, hydrogeochemical and copper isotopic analyses. Principal targeted Cu-minerals in the heap leaching process are covellite, bornite, and malachite. Resulting leached solution is of Mg-SO_4 type with high Al concentration, possibly as a consequence of micas alteration, mainly Mg-bearing muscovite, in extremely acid solution. The pH in the leachate was found to be 1.21 and the concentration of dissolved Cu present, mostly as $CuSO_4^0$ and Cu^{2+}, was about 2 g/L. Dissolved Al and Mg seem to behave conservatively, i.e., they do not precipitate, based on negative SI values for their minerals. In contrast, Ca and Fe concentrations can be controlled by precipitation of gypsum and jarosite, respectively, as suggested by the PHREEQC calculation results. Presence of these minerals in leached rocks was also confirmed by X-ray diffraction and scanning electron microscopy.

There is a strong depletion in heavy ^{65}Cu isotope of leached ore, with apparent isotopic fractionation $\Delta^{65}Cu_{leached\ ore\text{-}unleached\ ore}$ value of −4.54 ‰, and, in contrast, an isotopic enrichment in heavy ^{65}Cu isotope of the leaching solution with apparent isotopic fractionation $\Delta^{65}Cu_{leachate\text{-}unleached\ ore}$ value of +1.81 ‰. This is consistent with fractionation of $\delta^{65}Cu$ reported for dissolution of Cu-bearing minerals under controlled laboratory conditions and dissolved Cu in groundwater linked to porphyry copper deposits. To our knowledge, there was no previous study of Cu isotopes fractionation in the process of heap leaching. The leaching of heaps can be considered an analogy of leaching of gossans, although the supergene enrichment zone is missing due to extremely low pH and oxidizing conditions.

Table 3
Results of $\delta^{65}Cu$ analysis.

Sample	$\delta^{65}Cu$ [‰]	Comment	Principal Cu minerals
TS1A	−1.56	Unleached carbonate ore, 10% Cu	Malachite
TS1B	−2.45	Unleached carbonate ore, 5% Cu	Malachite, bornite
TS1C	−0.07	Unleached carbonate ore, 6% Cu	Malachite
TS2	1.42	Unleached carbonate ore, 15% Cu	Azurite, malachite
TS3	−8.17	Leached ore	
TS4	4.24	Metallic Cu, 89% Cu	Metallic Cu
TS5	−2.09	Unleached sulfide ore	Bornite, chalcopyrite
TS6	−4.11	Unleached carbonate ore	Malachite, bornite,
TS7	−3.87	Leached ore	
leachate	0.34	Leachate outflow	

CRediT authorship contribution statement

Ondra Sracek: Writing – original draft, Investigation, Formal analysis, Data curation, Conceptualization. **Vojtěch Ettler:** Writing – review & editing, Methodology, Formal analysis, Data curation. **Martin Mihaljevič:** Writing – review & editing, Project administration, Funding acquisition, Data curation. **Bohdan Kříbek:** Writing – review & editing, Formal analysis, Data curation. **Ben Mapani:** Writing – review & editing, Formal analysis, Data curation. **Vít Penížek:** Software, Resources, Formal analysis. **Tereza Zádorová:** Writing – review & editing, Data curation. **Aleš Vaněk:** Writing – review & editing, Formal analysis, Data curation.

Declaration of competing interest

Authors of submitted manuscript have no conflict of interest.

Acknowledgements

This study was supported by the Czech Science Foundation (GAČR project 23-05051S) and the Johannes Amos Comenius Programme (P JAC), project No. CZ.02.01.01/00/22_008/0004605, Natural and anthropogenic georisks. The staff of Consolidated Copper Co. (Tschudi copper mining operation) is acknowledged for providing the samples. We especially thank Mr. Josua Kalunde for facilitating the visit to the mine site. We thank many colleagues who helped with the analytical determinations: Marie Fayadová, Věra Vonásková and Lenka Jílková (bulk digestions and chemical analyses), Petr Drahota (XRD) and Martin Racek (SEM-EPMA).

Appendix A. Supplementary data

Supplementary data to this article can be found online at https://doi.org/10.1016/j.hydromet.2024.106356.

References

Albarède, F., 2004. The Stable Isotope Geochemistry of Copper and Zinc: Geochemistry of Non-Traditional Stable Isotopes, pp. 409–427.

Appelo, C.A.J., Postma, D., 2005. Geochemistry, Groundwater and Pollution, 2nd edition. A.A. Balkema Publishers, p. 649.

Bigalke, M., Weyer, S., Kobza, J., Wilcke, W., 2010. Stable cu and Zn isotope ratios as tracers of sources and transport of cu and Zn in contaminated soil. Geochim. Cosmochim. Acta 74, 6801–6813. https://doi.org/10.1016/j.gca.2010.08.044.

Bingöl, D., Canbazoğlu, M., 2004. Dissolution kinetics of malachite in sulphuric acid. Hydrometallurgy 72, 159–165. https://doi.org/10.1016/j.hydromet.2003.10.002.

Blowes, D.W., Ptacek, C.J., Jambor, J.L., Weisener, C.G., 2005. The geochemistry of acid mine drainage. In: Lollar, B.S. (Ed.), Environmental Geochemistry, Treatise on Geochemistry, vol. 9. Elsevier, pp. 149–204.

Braxton, D., Mathur, R., 2011. Exploration applications of copper isotopes in the supergene environment: a case study of the Bayugo porphyry copper-gold deposit, southern Philippines. Econ. Geol. 106, 1447–1463. https://doi.org/10.2113/econgeo.106.8.1447.

Bullen, T.D., Walczyk, T., 2009. Environmental and biomedical applications of natural metal stable isotope variations. Elements 5, 381–385. https://doi.org/10.2113/gselements.5.6.381.

Chapman, J.B., Mason, T.F.D., Weiss, D.J., Coles, B.J., Wilkinson, J.J., 2006. Chemical separation and isotopic variations of cu and Zn from five geological reference materials. Geostand. Geoanal. Res. 30 (1), 5–16. https://doi.org/10.1111/j.1751-908x.2006.tb00907.x.

Fernandez, A., Borrok, D.M., 2009. Fractionation of cu, Fe, and Zn isotopes during the oxidative weathering of sulfide-rich rocks. Chem. Geol. 264, 1–12. https://doi.org/10.1016/j.chemgeo.2009.01.024.

Gražulis, S., Daškevič, A., Merkys, A., Chateigner, D., Lutterotti, L., Quirós, M., Serebryanaya, N.R., Moeck, P., Downs, R.T., Le Bail, A., 2012. Crystallography open database (COD): an open-access collection of crystal structures and platform for world-wide collaboration. Nucleic Acids Res. 40, D420–D427. https://doi.org/10.1093/nar/gkr900.

Hradil, D., Hostomský, J., 2002. Effect of composition and physical properties of natural kaolinitic clays on their strong acid weathering rates. Catena 171-181. https://doi.org/10.1016/S0341-8162(02)00024-3.

Kim, Y., Lee, I., Oyungerel, S., Jargal, L., Tsedenbal, T., 2019. Cu and S isotopic signatures of the Erdenetiin Ovoo porphyry cu-Mo deposit, northern Mongolia: implications for their origin and mineral exploration. Ore Geol. Rev. 104, 656–669.

Klein, S., Brey, P.G., Durali-Muller, S., Lahaye, Y., 2010. Characterisation of the raw metal sources used for the production of copper and copper-based objects with copper isotopes. Archeol. Anthropol. Sci 2, 45–56. https://doi.org/10.1007/s12520-010-0027-y.

Kříbek, B., Zachariáš, J., Knésl, I., Míková, J., Mihaljevič, M., Veselovský, F., Bamba, O., 2016. Geochemistry, mineralogy, and isotope composition of Pb, Zn, and cu in primary ores, gossan and barren ferruginous crust from the Perkoa base metal deposit, Burkina Faso. J. Geochim. Explor. 168, 49–64. https://doi.org/10.1016/j.gexplo.2016.05.007.

Kříbek, B., Šípková, A., Ettler, V., Mihaljevič, M., Majer, V., Knésl, I., Mapani, B., Penížek, V., Vaněk, A., Sracek, O., 2018. Variability of the copper isotopic composition in soil and grass affected by mining and smelting in Tsumeb, Namibia. Chem. Geol. 493, 121–135. https://doi.org/10.1016/j.chemgeo.2018.05.035.

Lefebvre, R., Hockley, D., Smolensky, J., Gélinas, P., 2001. Multiphase transfer processes in waste rock piles producing acid mine drainage: 1: conceptual model and system characterization. J. Contam. Hydrol. 52 (1–4), 137–164. https://doi.org/10.1016/S0169-7722(01)00156-5.

Lwambiyi, M., Maweja, K., Kongolo, K., Lwambiyi, N.M., Diyambi, M., 2009. Investigation into the heap leaching of copper ore from the Disele deposit. Hydrometallurgy 98, 177–180. https://doi.org/10.1016/j.hydromet.2009.04.016.

Maghsoudy, S., Bakhtiari, O., Maghsoudy, S., 2022. Tortuosity prediction and investigation of fluid flow behavior using pore flow approach in heap leaching. Hydrometallurgy 211, 105868. https://doi.org/10.1016/j.hydromet.2022.105868.

Mahan, B., Mathur, R., Sanislav, I., Rea, P., Dirks, P., 2023. Cu isotopes in groundwater for hydrogeochemical mineral exploration: a case study using the world-class Mount Isa cu–Pb–Zn deposit (Australia). Appl. Geochem. 148, 105519 https://doi.org/10.1016/j.apgeochem.2022.105519.

Majzlan, J., Mathur, R., Milovský, R., Milovská, S., 2022. Isotopic exchange of oxygen, sulfur, hydrogen and copper between aqueous phase and the copper minerals brochantite, libethenite and olivenite. Mineral. Mag. 86, 644–651. https://doi.org/10.1180/mgm.2021.77.

Markl, G., Lahaye, Y., Schwinn, G., 2006. Copper isotopes as monitors of redox processes in hydrothermal mineralization. Geochim. Cosmochim. Acta 70, 4215–4228. https://doi.org/10.1016/j.gca.2006.06.1369.

Mathur, R., Fantle, M.S., 2015. Copper isotopic perspectives on supergene processes: implications for the global cu cycle. Elements 11, 323–329. https://doi.org/10.2113/gselements.11.5.323.

Mathur, R., Schlitt, W.J., 2010. Identification of the dominant cu ore minerals providing soluble copper at Cañariaco, Peru through Cu isotope analyses of batch leach experiments. Hydrometallurgy 101, 15–19. https://doi.org/10.1016/j.hydromet.2009.11.005.

Mathur, R., Ruiz, J., Titley, S., Liermann, L., Buss, H., Brantley, S.L., 2005. Cu isotopic fractionation in the supergene environment with and without bacteria. Geochim. Cosmochim. Acta 69, 5233–5246. https://doi.org/10.1016/j.gca.2005.06.022.

Mendelsohn, J., Jarvis, A., Roberts, C., Robertson, T., 2002. Atlas of Namibia: A Portrait of Land and its People, vol. 53. David Philip Publisher. https://doi.org/10.1017/CBO9781107415324.004.

Mihaljevič, M., Baieta, R., Ettler, V., Vaněk, A., Kříbek, B., Penížek, V., Drahota, P., Trubač, J., Sracek, O., Chrastný, V., Mapani, B.S., 2019. Tracing of the metal dynamics in semi-arid soils near mine tailings using stable cu and Pb isotopes. Chem. Geol. 515, 61–76. https://doi.org/10.1016/j.chemgeo.2019.03.026.

Nicol, M.J., 2018. The kinetics of the dissolution of malachite in acid solutions. Hydrometallurgy 177, 214–217. https://doi.org/10.1016/j.hydromet.2018.03.017.

Parkhurst, D.L., Appelo, C.A.J., 1999. Guide to PHREEQC (Version 2)-A Computer Program for Speciation, Batch-reaction, One-Dimensional Transport, and Inverse Geochemical Calculations, Water-Resources Investigations Report 99–4259. U.S. Geological Survey.

Petersen, J., 2016. Heap leaching as a key technology for recovery of values from low-grade ores - a brief overview. Hydrometallurgy 165, 206–212. https://doi.org/10.1016/j.hydromet.2018.03.017.

Plumhoff, A.M., Mathur, R., Milovský, R., Majzlan, J., 2021. Fractionation of the copper, oxygen and hydrogen isotopes between malachite and aqueous phase. Geochim. Cosmochim. Acta 300, 246–257. https://doi.org/10.1016/j.gca.2021.02.009.

Qi, D., Behrens, H., Lazarova, M., Weyer, S., 2019. Cu isotope fractionation during reduction processes in aqueous systems: evidences from electrochemical deposition. Contrib. Mineral. Petrol. 174, 37. https://doi.org/10.1007/s00410-019-1568-4.

Sarjoughian, F., Shubin, F., Asadi, S., Moore, F., Haschke, M., 2024. Cu isotope patterns of whole rocks in the Kerman porphyry copper belt, southeastern Urumieh Dokhtar magmatic arc, Iran. J. Geochem. Explor. 256, 107329 https://doi.org/10.1016/j.gexplo.2023.107329.

Schneider, G., 2008. The Roadside Geology of Namibia. Gerbruder Bortnaeger, Berlin, Stuttgart.

Sracek, O., Choquette, M., Gélinas, P., Lefebvre, R., Nicholson, R.V., 2004. Geochemical characterization of acid mine drainage from a waste rock pile, mine Doyon, Québec, Canada. J. Contam. Hydrol. 69 (1–2), 45–71. https://doi.org/10.1016/S0169-7722(03)00150-5.

Thomas, M., 2021. Understanding gangue acid consumption in copper sulfide heap leaching: predicting the impact of carbonates, silicates and secondary precipitates. Miner. Eng. 171, 107090 https://doi.org/10.1016/j.mineng.2021.107090.

Van Wyk, A.E., Strub, H., Struckmeir, W.F., 2001. Hydrogeological Map of Namibia. Department of Water Affairs/Geological Survey, Windhoek, Namibia.

Wall, A.J., Mathur, R., Post, J.E., Heaney, P.J., 2011. Cu isotope fractionation during bornite dissolution: an in situ X-ray diffraction analysis. Ore Geol. Rev. 42, 62–70. https://doi.org/10.1016/j.oregeorev.2011.01.001.

Warr, L.N., 2021. IMA-CNMNC approved mineral symbols. Mineral. Mag. 85, 291–320. https://doi.org/10.1180/mgm.2021.43.

Watling, H.R., 2006. The bioleaching of sulphide minerals with emphasis on copper sulphides - a review. Hydrometallurgy 84, 81–102. https://doi.org/10.1016/j.hydromet.2006.05.001.

Wiederhold, J.G., 2015. Metal stable isotope signatures as tracers in environmental geochemistry. Environ. Sci. Technol. 49, 2606–2624. https://doi.org/10.1021/es504683e.